- Supplementary Information -

Amplified Arctic warming by phytoplankton under greenhouse warming

Jong-Yeon Park[1], Jong-Seong Kug[2], Jürgen Bader[1,3], Rebecca Rolph[1,4] , and Minho Kwon[5]

[1]Max Planck Institute for Meteorology, Hamburg, Germany

[2]School of Environmental Science and Engineering, Pohang University of Science and Technology (POSTECH), Pohang, South Korea

[3]Uni Climate, Uni Research & the Bjerknes Centre for Climate Research, Bergen, Norway

[4]University of Hamburg, Klimacampus, Hamburg, Germany

[5]Korea Institute of Ocean Science and Technology, Ansan, South Korea

Direct biological impact on oceanic shortwave heating (OGCM Experiments)

The bio-geophysical influence considered in this study is the role of marine phytoplankton in modifying the vertical distribution of oceanic shortwave heating. Phytoplankton and their derivatives are acknowledged to be important factors in determining the optical properties of ocean water, which leads to a surface warming and subsurface cooling through the increased attenuation of downwelling solar radiation[1]. This first-order biological heating change is quantitatively examined from a supplementary experiment using an ocean-only model coupled with a biogeochemical model. These are ocean and biogeochemical components of the fully coupled climate model, which is used in our main analysis. Here, the advantage of using an ocean-only model rather than a fully-coupled model is that the direct impact of biological heating can be estimated by excluding the secondary indirect impact caused by ocean-atmosphere interactions, which may mask or overshadow the direct biological heating effect[2-

[4]. The boundary data for the ocean-only model experiment are the historical (1951-2010) winds provided by the National Centers for Environmental Prediction-National Center for Atmospheric Research (NCEP-NCAR) reanalysis 1[5] and the climatological heat fluxes from the Common Ocean-Ice Reference Experiment (CORE) data[6]. Two parallel runs are conducted by turning the biogeochemical model on and off, which is a similar set-up to that used in our main experiments. That is, interactive chlorophyll simulated from the biogeochemical model is used for the calculation of oceanic shortwave heating in one experiment (Ocean.ECO.on), whereas in the other experiment (Ocean.ECO.off), the chlorophyll is prescribed by setting it to zero, which mimics optically pure ocean water. In the Arctic region (0^{o}-360^{o}E; 65^{o}~90^{o}N), the vertical distribution of simulated chlorophyll shows its maximum concentration at around 50-m depth where both solar radiation and nutrients for phytoplankton growth are sufficient (green line in Fig. S1a). As widely known, such feature is the natural consequence of light-limited phytoplankton growth in the deep layer and nutrient-limited growth in the upper mixed layer[7,8]. The presence of phytoplankton in Ocean.ECO.on results in more shortwave heating in the upper ocean above 30-m depth and less heating below 30-m depth compared to Ocean.ECO.off (Fig. S1b). The total biological heating in the upper ocean is ~5.9 W/m^2, which accounts for about 9% of total shortwave flux coming into Arctic Ocean. This is the basic assumption of phytoplankton-shortwave penetration feedback considered in our study.

Global pattern of biologically-induced warming

Two transient carbon dioxide (CO_2) warming experiments with and without interactive bio-geophysical feedback (i.e. ECO.on and ECO.off, respectively) show that the simulated future surface warming is intensified in the experiment with interactive bio-geophysical feedback (Fig S2). The intensified surface warming is most prominent in the Arctic, the main focus of this study, but there is also a modest warming in mid-latitude and tropics. Unlike the intensified Arctic warming that coincides with an increase in phytoplankton, the warming in low latitudes cannot be straightforwardly explained by the future phytoplankton change, owing to a decrease in phytoplankton over most of the subtropics and tropics. A detailed analysis of the source of the low latitudes warming is beyond the scope of this study, but we found that the warming in the low latitude is likely to be triggered by the Arctic warming. As shown in the time evolution of zonally-averaged difference in surface temperature between ECO.on and ECO.off, the Arctic warming seems to be followed by low latitudes warming (Fig. S3). This suggests that the intensified Arctic warming may not be triggered by a remote influence from low latitudes, but by a local process confined to Arctic regions.

Seasonal variation in biologically-triggered Arctic climate change

The intensified Arctic warming considering the future changes in chlorophyll is investigated on a seasonal time scale. The amplified surface warming in ECO.on than in ECO.off appears to be the strongest in winter season and the weakest in summer (Fig. S4). The warming pattern is tightly linked to the decline in sea ice concentration in the Arctic. The sea ice reduction largely occurs in regions where the surface warming is strong, particularly near the Kara Sea and Chukchi Sea in winter and spring (Fig. S5). These areas are generally the marginal regions of Arctic sea ice in these seasons. In summer and fall, however, most of the Arctic Ocean becomes an ice-free area under doubled CO_2, and thus the additional sea ice decline by biological feedback appears over a wider area, but with a subtle decline in magnitude. One thing to note here is that although the amount of sea ice reduction is similar in both winter and spring, the surface warming is much stronger in winter than in spring. This is especially interesting because the stronger chlorophyll bloom in spring may trigger the stronger biological warming in the ocean surface (Fig. S6b). The reason for the strong winter warming is that the ocean plays a role as a heat sink in summer, and as a heat source in winter. That is, in summer, the excess energy is used to warm the upper ocean and melt sea ice, but in winter, this heat is released to the atmosphere, and thus leads to a greater surface warming. The mechanism of the strong winter temperature response due to the seasonal reversal of atmosphere-ocean heat flux in Arctic is previously addressed in examining the role of sea ice in Arctic amplification or the atmospheric response to Arctic Sea ice loss[9-11].

Similar experiments using another climate model

The robustness of the enhanced Arctic warming linked to the future phytoplankton change is further tested using another state-of-the-art climate model, the fully-coupled Max Planck Earth System model (MPI-ESM). With this model, we carried out two global warming experiments similar to our main experiments of GFDL CM2.1. The two warming experiments using MPI-ESM are also prescribed by CO_2, increased by 1% per year to double its initial concentration, and run for 100 years. To produce a simple representation of future phytoplankton change, we prescribed different optical types of water in the two warming experiments instead of using interactive and prescribed chlorophyll. That is, in one experiment, an optically clear water type is prescribed (which is comparable with the experiment 'ECO.off' in the main manuscript) in regions where sea ice melts under CO_2 warming, compared to the present climate simulation, while in the other warming experiment, a 'dirty' water type is prescribed (which is comparable with 'ECO.on') in the same ice-melting regions. Here, the so-called Jerlov optical water type IA and water type III are used for the optically clean and dirty water, respectively[15]. The reasoning behind the setup of this supplementary experiment begins with the fact that when the sea ice retreats under an increasing CO_2 scenario and the ocean surface beneath the ice is consequently exposed to shortwave radiation, phytoplankton have better light conditions for growth than before.

The differences in surface warming and sea ice concentration between the type IA and III experiment are found in Fig. S12. The increased water turbidity in sea-ice melting regions appears to cause a substantial additional warming in the Arctic. The magnitude of warming is similar to the biologically-induced Arctic warming shown in Fig. 2a in the main manuscript. Interestingly, the most prominent regions showing an increase in surface temperature and a decline in sea ice concentration can be found near the Kara Sea, which corresponds with the result from our main experiment. This result reaffirms our conclusion on the role of future phytoplankton change in amplifying future Arctic warming through the modification of oceanic optical property.

References

1 Lewis, M. R., Carr, M. E., Feldman, G. C., Esaias, W. & McClain, C. Influence of penetrating solar-radiation on the heat-budget of the equatorial Pacific-ocean. *Nature* **347**, 543-545 (1990).

2 Loptien, U., Eden, C., Timmermann, A. & Dietze, H. Effects of biologically induced differential heating in an eddy-permitting coupled ocean-ecosystem model. *J. Geophys. Res.* **114**, C06011 (2009).

3 Manizza, M., Le Quéré, C., Watson, A. J. & Buitenhuis, E. T. Bio-optical feedbacks among phytoplankton, upper ocean physics and sea-ice in a global model. *Geophys. Res. Lett.* **32** (2005).

4 Park, J.-Y., Kug, J.-S., Seo, H. & Bader, J. Impact of bio-physical feedbacks on the tropical climate in coupled and uncoupled GCMs. *Clim. Dyn.*, 1-17 (2013).

5 Kalnay, E. *et al.* The NCEP/NCAR 40-year reanalysis project. *Bul. Am. Meteorol. Soc.* **77**, 437-471 (1996).

6 Large, W. & Yeager, S. Diurnal to decadal global forcing for ocean and sea-ice models: The data sets and flux climatologies. (Natl. Cent. for Atmos. Res., Boulder, Colo, 2004).

7 Bienfang, P. & Gundersen, K. Light effects on nutrient-limited, oceanic primary production. *Marine Biology* **43**, 187-199 (1977).

8 Russell, F. S. The vertical distribution of plankton in the sea. *Biological Reviews and Biological Proceedings of the Cambridge Philosophical Society* **2**, 213-262 (1927).

9 Deser, C., Tomas, R., Alexander, M. & Lawrence, D. The Seasonal Atmospheric Response to Projected Arctic Sea Ice Loss in the Late Twenty-First Century. *J. Clim.* **23**, 333-351 (2010).

10 Screen, J. A. & Simmonds, I. The central role of diminishing sea ice in recent Arctic temperature amplification. *Nature* **464**, 1334-1337 (2010).

11 Tietsche, S., Notz, D., Jungclaus, J. H. & Marotzke, J. Recovery mechanisms of Arctic summer sea ice. *Geophys. Res. Lett.* **38** (2011).

12 Khodri, M. *et al.* Simulating the amplification of orbital forcing by ocean feedbacks in the last glaciation. *Nature* **410**, 570-574 (2001).

13 Manabe, S. & Wetherald, R. T. On the distribution of climate change resulting from an increase in CO2 content of the atmosphere. *J. Atmos. Sci.* **37**, 99-118 (1980).

14 Spielhagen, R. F. *et al.* Enhanced Modern Heat Transfer to the Arctic by Warm Atlantic Water. *Science* **331**, 450-453 (2011).

15 Jerlov, N. G. Marine optics. *Elsevier oceanogr* **14**, i-xiii,1-231 (1976).

Table S1. The length of open water season (unit: day) in different Arctic areas: Barents (30°-60°E, 65°-75°N), Kara (60°-90°E, 70°-80°N), Laptev (100°-150°E, 75°-80°N), Siberian (150°-180°E, 70°-80°N), and Chukchi (180°-170°W, 65°-75°N). The open water season is defined as the number of days when sea ice concentration is lower than 5%.

	ECO.off	ECO.on	ECO.on – ECO.off
Barents	245	311	+66
Kara	141	163	+22
Laptev	100	103	+3
Siberian	97	108	+11
Chukchi	153	172	+19

Figures

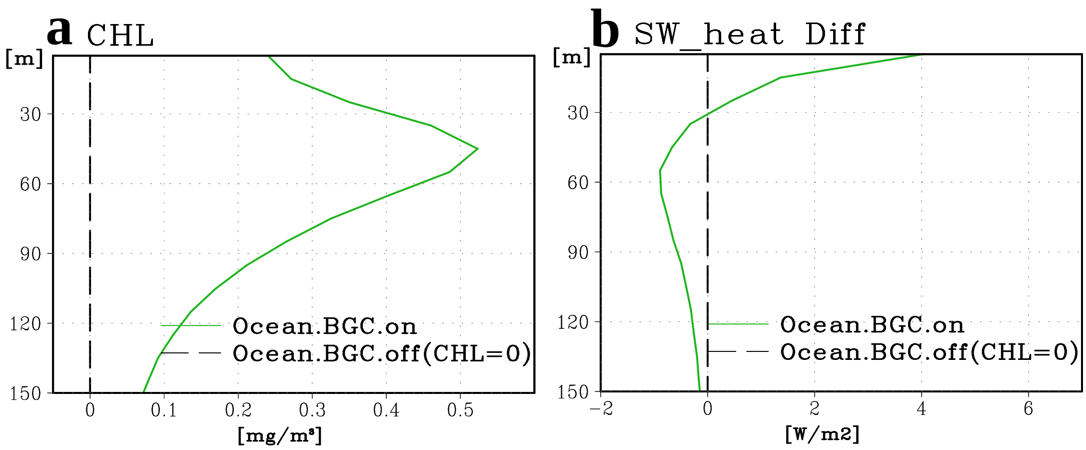

Figure S1. Vertical profile of chlorophyll (**a**) and oceanic shortwave heating (**b**) in Arctic (0-360°E; 65°-90°N) simulated in two experiments with and without chlorophyll, i.e. Ocean.ECO.on (green-solid line), and Ocean.ECO.off (black-dashed line). The shortwave heating in (**b**) is presented as the difference from Ocean.ECO.off.

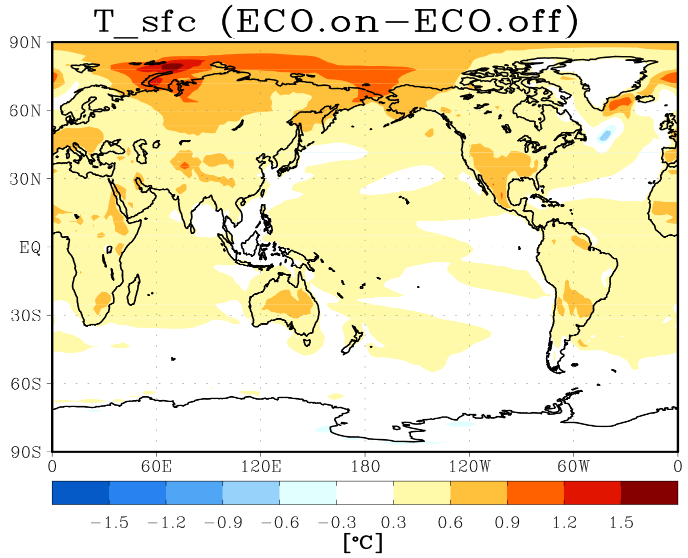

Figure S2. Five-member ensemble mean difference of surface temperature between two experiments, ECO.on and ECO.off, with and without interactive biological feedback to oceanic shortwave heating. This is the same as Figure 2a in the main manuscript, but in a global map.

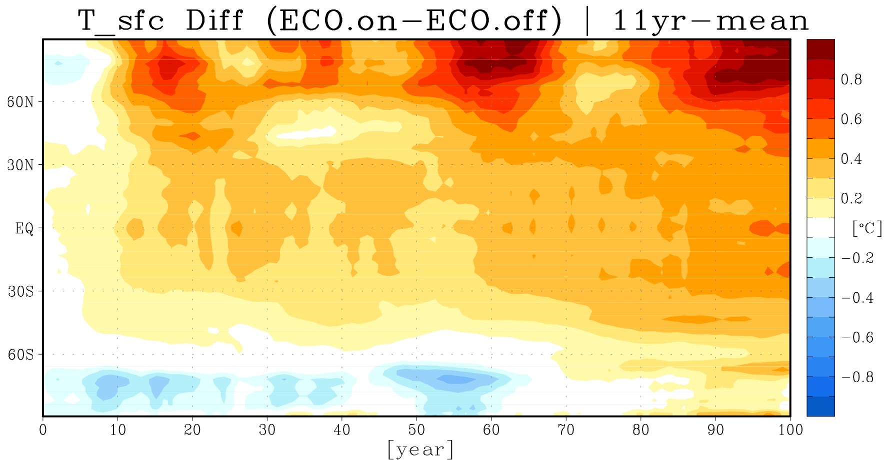

Figure S3. The time evolution of zonal mean (0-360°E) difference in surface temperature between ECO.on and ECO.off. The difference is calculated from five-member ensemble runs and smoothed using an eleven-year running mean.

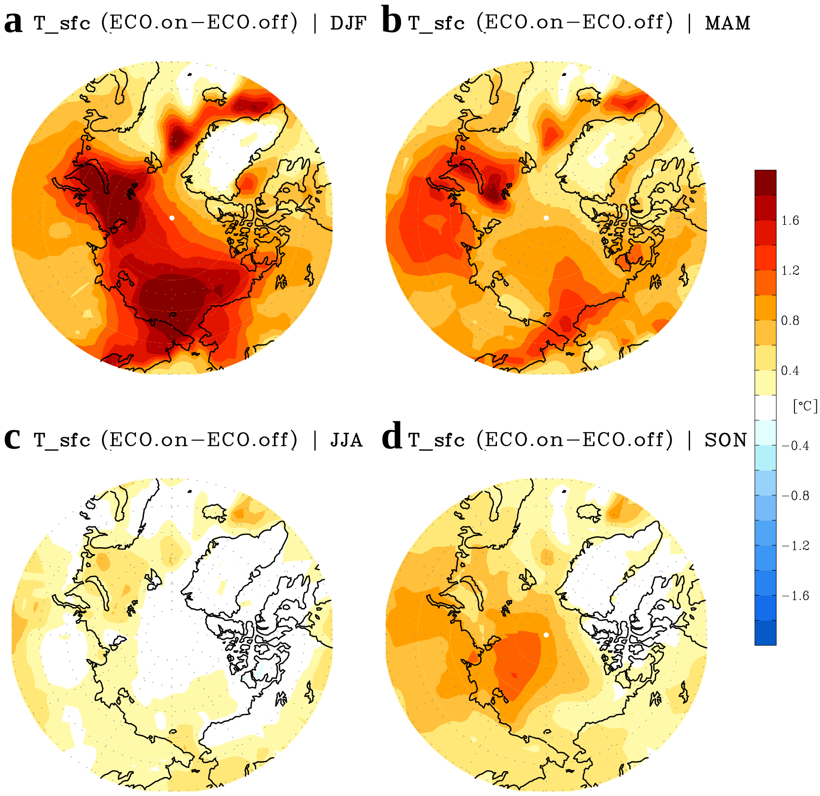

Figure S4. Difference in mean surface temperature between two CO_2 warming experiments with and without interactive bio-geophysical feedback in DJF (**a**), MAM (**b**), JJA (**c**), and SON (**d**).

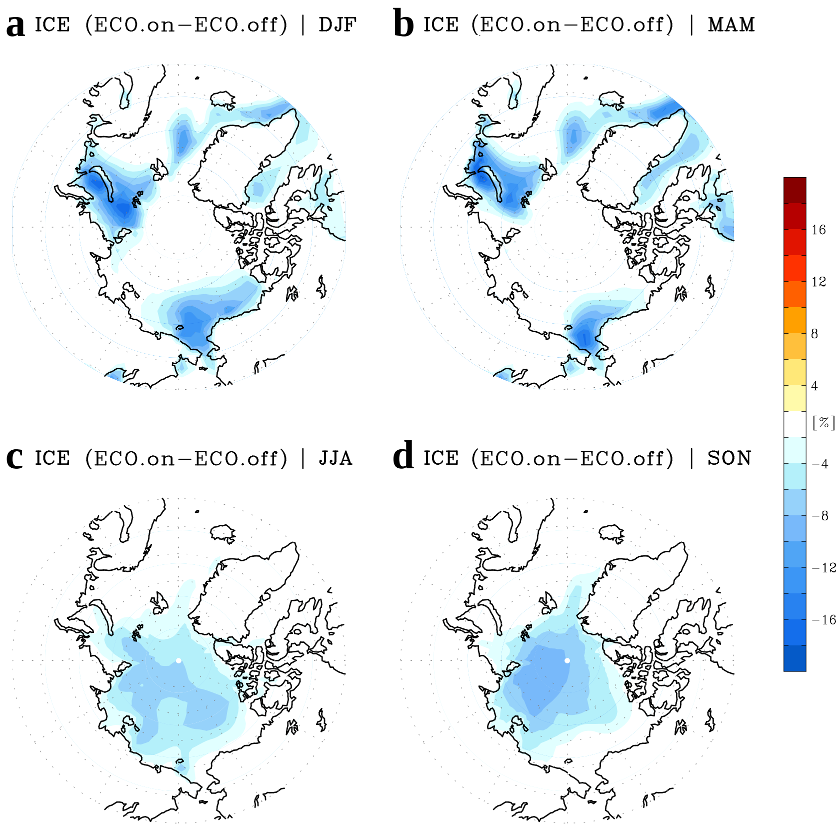

Figure S5. Same as Fig. S4 but for sea ice concentration.

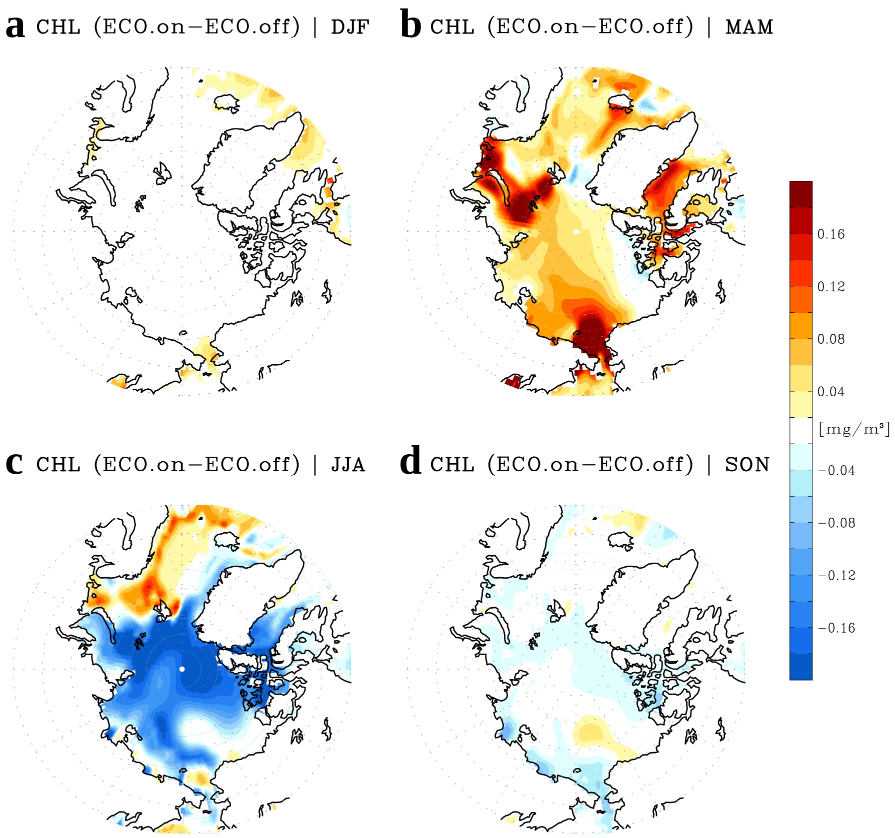

Figure S6. Same as Fig. S4 but for chlorophyll concentration averaged in the upper 30-m ocean.

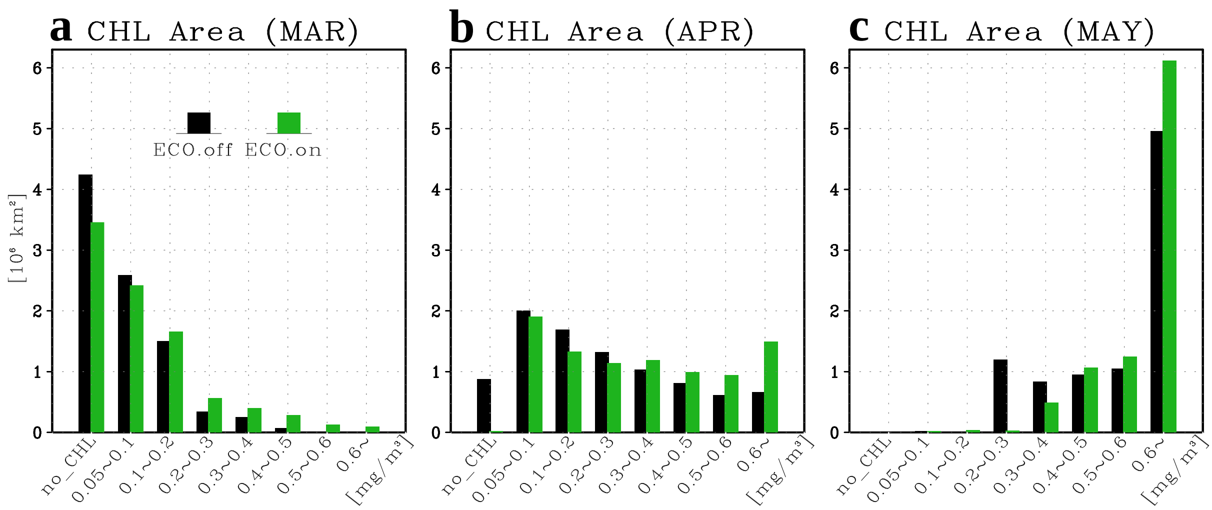

Figure S7. The area within different ranges of chlorophyll concentration in the Arctic (30^{o}W-210^{o}E, 65^o-90^{o}N) simulated by ECO.off (black bar) and ECO.on (green bar).

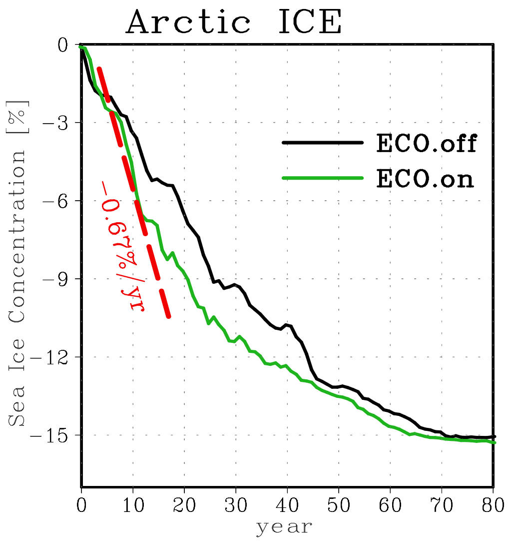

Figure S8. Time evolution of Arctic (0-360°E; 75°-90°N) sea-ice concentrations anomalies (with respect to the long-term mean of present-day simulation, i.e. ECO.on_1xCO2) simulated by two warming climate simulations, ECO.off (black line) and ECO.on (green line). Both simulations project the disappearance of perennial sea ice after 70 years. The data are September mean values when sea-ice coverage is at its minimum, and are smoothed using a 15-year running mean. The red-dashed line represent the observed decline rate of Arctic sea-ice concentration during 1990-2010.

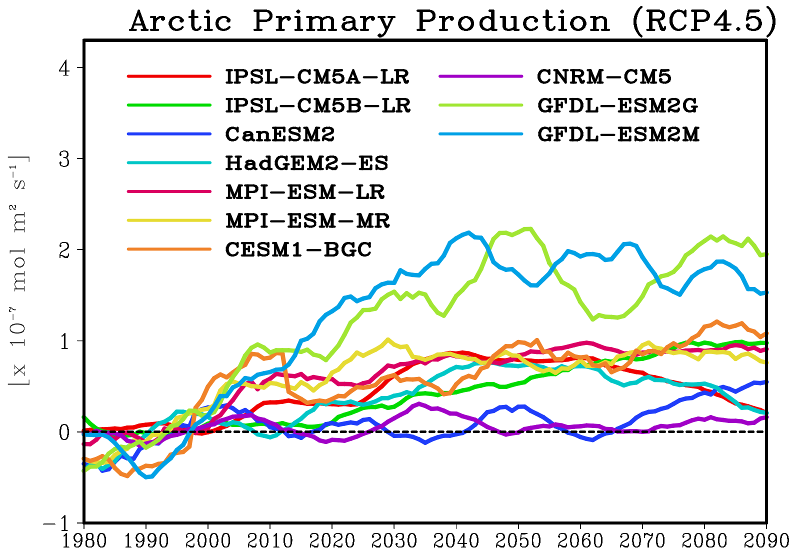

Figure S9. The anomalies of total primary (organic carbon) production by Arctic phytoplankton from 10 climate models in CMIP5. The anomalies are the differences from the 1980-2005 mean. The historical and a climate change scenario (the representative concentration pathway 4.5) are used. All the time series data are smoothed using a 15-year running mean and all available ensemble members are used for each model.

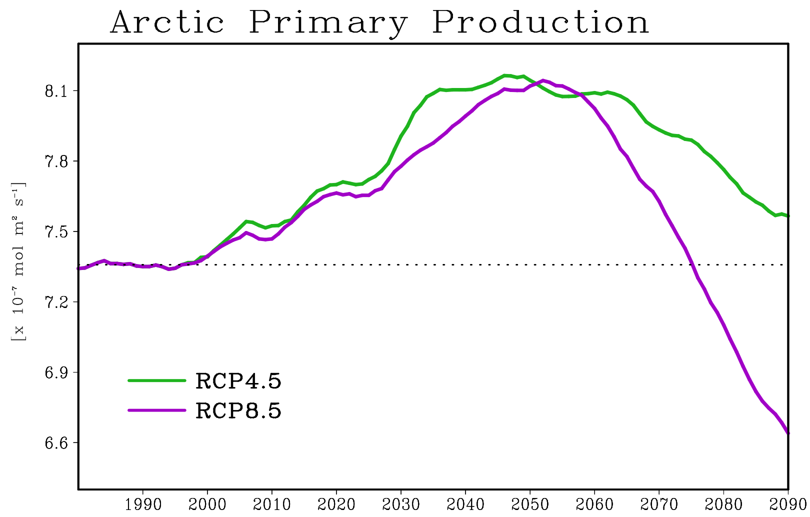

Figure S10. Temporal evolution of Arctic primary production in historical (6 ensemble mean) and future scenario (4 ensemble mean) simulations from IPSL-CM5A-LR. The green line represents the simulation under the representative concentration pathway (RCP) 4.5, a modest climate change scenario, and the purple line represents the RCP 8.5 simulation, the strongest climate change scenario in CMIP5. The dotted line indicates the level of production in 1980-2000.

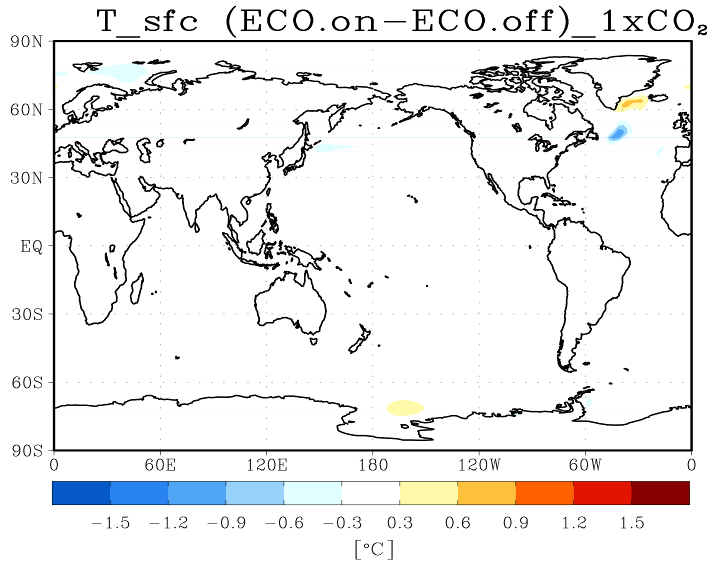

Figure S11. Mean difference of surface temperature between two 300-year-long present climate experiments, ECO.on_1xCO2 and ECO.off_1xCO2, with and without interactive bio-geophysical feedback.

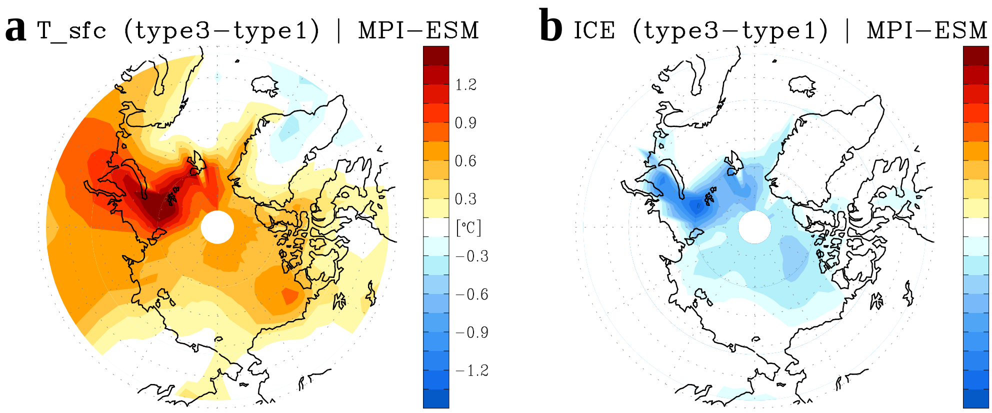

Figure S12. The annual mean difference of surface temperature (**a**) and sea ice concentration (**b**) between two supplementary CO_2 warming experiments prescribed by low and high turbidity of water in sea-ice melting regions. The experiments are conducted using MPI-ESM, and Jerlov optical water type IA and type III are prescribed.